Possibilities of the particle finite element method for fluid-structure interaction problems with free surface waves

Eugenio Oñate[⋆] — **Sergio Rodolfo Idelsohn**[⋆,⋆⋆]
Facundo Del Pin[⋆,⋆⋆] — **Romain Aubry**[⋆]

[⋆] *International Center for Numerical Methods in Engineering (CIMNE)*
Universidad Politecnica de Cataluna, Campus Norte UPC, 08034 Barcelona, Spain
onate@cimne.upc.es

[⋆⋆] *CIMEC, Universidad Nacional del Litoral, Güemes 3450, 3000 Santa Fe, Argentina*
sergio@ceride.gov.ar

ABSTRACT. *We present a general formulation for analysis of fluid-structure interaction problems using the particle finite element method (PFEM). The key feature of the PFEM is the use of a Lagrangian description to model the motion of nodes (particles) in both the fluid and the structure domains. Nodes are thus viewed as particles which can freely move and even separate from the main analysis domain representing, for instance, the effect of water drops. A mesh connects the nodes defining the discretized domain where the governing equations, expressed in an integral from, are solved as in the standard FEM. The necessary stabilization for dealing with the incompressibility condition in the fluid is introduced via the finite calculus (FIC) method. A fractional step scheme for the transient coupled fluid-structure solution is described. Examples of application of the PFEM method to solve a number of fluid-structure interaction problems involving large motions of the free surface and splashing of waves are presented.*

RÉSUMÉ. *On présente une formulation générale pour l'analyse de problèmes d'interaction fluide-structure fondée sur la méthode des éléments finis particulaires (MEFP). L'aspect essentiel de la MEFP est la représentation lagrangienne du mouvement des noeuds dans les domaines fluide et structure. Les noeuds sont ainsi vus comme des particules qui peuvent se mouvoir librement et même se séparer du domaine principal d'analyse modélisation de gouttes d'eau). Un maillage connecte les noeuds définissant le domaine discrétisé sur lequel les équations de champ, écrites sous forme intégrale, sont résolues comme avec la méthode des éléments finis classique. La nécessaire stabilisation permettant la prise en compte de la condition d'incompressibilité dans le fluide est introduite via l'analyse finie. Un schéma à pas fractionnaire pour le problème d'évolution fluide-structure couplé est décrit. Des exemples d'application de la MEFP à des problèmes d'interaction avec grands mouvements de surface libre et aspersion par vagues sont présentés.*

KEYWORDS: *particle finite element method; finite element method; fluid-structure interaction; finite calculus*

MOTS-CLÉS : *méthode des éléments finis particulaires ; méthode des éléments finis ; interaction fluide-structure ; analyse finie*

REEF – 13/2004. Giens 2003, pages 637 to 666

1. Introduction

There is an increasing interest in the development of robust and efficient numerical methods for analysis of engineering problems involving the interaction of fluids and structures accounting for large motions of the fluid free surface and the existance of fully or partially submerged bodies. Examples of this kind are common in ship hydrodynamics, off-shore structures, spillways in dams, free surface channel flows, liquid containers, stirring reactors, mould filling processes, etc.

The movement of solids in fluids is usually analyzed with the finite element method (FEM) [ZIE 00] using the so called arbitrary Lagrangian-Eulerian (ALE) formulation [DON 03]. In the ALE approach the movement of the fluid particles is decoupled from that of the mesh nodes. Hence the relative velocity between mesh nodes and particles is used as the convective velocity in the momentum equations.

Typical difficulties of fluid-structure interaction (FSI) analysis using the FEM with both the Eulerian and ALE formulation include the treatment of the convective terms and the incompressibility constraint in the fluid equations, the modelling and tracking of the free surface in the fluid, the transfer of information between the fluid and solid domains via the contact interfaces, the modelling of wave splashing, the possibility to deal with large rigid body motions of the structure within the fluid domain, the efficient updating of the finite element meshes for both the structure and the fluid, etc.

Most of these problems disappear if a *Lagrangian description* is used to formulate the governing equations of both the solid and the fluid domain. In the Lagrangian formulation the motion of the individual particles is followed and, consequently, nodes in a finite element mesh can be viewed as moving "particles". Hence, the motion of the mesh discretizing the total domain (including both the fluid and solid parts) is followed during the transient solution.

In this paper we present a particular class of Lagrangian formulation to solve problems involving the interaction between fluids and solids in a unified manner. The method, called the *particle finite element method* (PFEM), treats the mesh nodes in the fluid and solid domains as particles which can freely move an even separate from the main fluid domain representing, for instance, the effect of water drops. A finite element mesh connects the nodes defining the discretized domain where the governing equations are solved in the standard FEM fashion. The PFEM is the natural evolution of recent work of the authors for the solution of FSI problems using Lagrangian finite element and meshless methods [AUB 04, IDE 03, IDE 03B, IDE 04, ONA 03, ONA 04B].

An advantage of the Lagrangian formulation is that the convective terms do not enter in the fluid equations. The difficulty is however transferred to the problem of adequately (and efficiently) moving the mesh nodes. Indeed for large mesh motions remeshing may be a frequent necessity along the time solution. We use an innovative mesh regeneration procedure blending elements of different shapes using an extended Delaunay tesselation [IDE 03, IDE 03C].

The layout of the paper is the following. In the next section the basic ideas of the PFEM are outlined. Next the basic equation for an incompressible flow using a

Lagrangian description and a finite calculus (FIC) formulation are presented. Then a fractional step scheme for the transient solution via standard finite element procedures is described. Details of the treatment of the coupled FSI problem are given. The procedures for mesh generation and for identification of the free surface nodes are briefly outlined. Finally, the efficiency of the *particle finite element method* (PFEM) is shown in its application to a number of FSI problems involving large flow motions, surface waves, moving bodies. etc.

2. Rationale of the Particle Finite Element Method

In the PFEM approach presented here, both the fluid and the solid domains are modelled using an *updated Lagrangian formulation*. The finite element method (FEM) is used to solve the continuum equations in both domains. Hence a mesh discretizing these domains must be generated in order to solve the governing equations for both the fluid and solid problems in the standard FEM fashion. We note once more that the nodes discretizing the fluid and solid domains can be viewed as material particles which motion is tracked during the transient solution.

The quality of the numerical solution obviously depends on the discretization chosen as in the standard FEM. Adaptive mesh refinement techniques can be used to improve the solution in zones where large motions of the fluid or the structure occur.

The Lagrangian formulation allows to track the motion of each single fluid particle (a node). This is useful to model the separation of water particles from the main fluid domain and to follow their subsequent motion as individual particles with an initial velocity and subject to gravity forces.

In summary, a typical solution with the PFEM involves the following steps.

1) Discretize the fluid and solid domains with a finite element mesh. For the mesh generation process we use and extended Delaunay technique (see Section 8) starting with an initial collection of points which then become the mesh nodes.

2) Identify the external boundaries for both the fluid and solid domains. This is an essential step as some boundaries (such as the free surface in fluids) may be severely distorted during the solution process including separation and re-entring of nodes. The Alpha Shape method [EDE 99] is used for the boundary definition (see Section 9).

3) Solve the coupled Lagrangian equations of motion for the fluid and the solid domains. Compute the relevant state variables in both domains at each time step: velocities, pressure and viscous stresses in the fluid and displacements, stresses and strains in the solid.

4) Move the mesh nodes to a new position in terms of the time increment size. This step is typically a consequence of the solution process of step 3.

5) Generate a new mesh if needed. The mesh regeneration process can take place after a prescribed number of time steps or when the actual mesh has suffered severe distosions due to the Lagrangian motion. In our work we use an innovative

mesh generation scheme based on the extended Delaunay tesselation (Section 7) [IDE 03, IDE 03B, IDE 04].

6) Go back to step 2 and repeat the solution process for the next time step.

Details of the stabilized Lagrangian FEM for the solution of the fluid equations using a FIC formulation are presented in the next section. The fractional scheme chosen for the transient coupled FSI solution using the FEM and details of the boundary recognition method and the mesh regeneration process are given in subsequent sections. Finally some examples of application of the PFEM are given.

3. Lagrangian equations for an incompressible fluid. FIC formulation

The standard infinitesimal equations for a viscous incompressible fluid can be written in an updated Lagrangian frame as [ONA 98, ZIE 00]

Momentum

$$r_{m_i} = 0 \quad \text{in } \Omega \tag{1}$$

Mass balance

$$r_d = 0 \quad \text{in } \Omega \tag{2}$$

where

$$r_{m_i} = \rho \frac{\partial v_i}{\partial t} + \frac{\partial \sigma_{ij}}{\partial x_j} - b_i \tag{3}$$

$$r_d = \frac{\partial v_i}{\partial x_i} \qquad i,j = 1, n_d \tag{4}$$

Above n_d is the number of space dimensions, v_i is the velocity along the ith global axis, ρ is the (constant) density of the fluid, b_i are the body forces and σ_{ij} are the total stresses given by

$$\sigma_{ij} = s_{ij} - \delta_{ij} p \tag{5}$$

where p is the absolute pressure (defined positive in compression). As usual the deviatoric stresses s_{ij} are related to the viscosity by the standard expression

$$s_{ij} = 2\mu \left(\dot{\varepsilon}_{ij} - \delta_{ij} \frac{1}{3} \frac{\partial v_k}{\partial x_k} \right) \tag{6}$$

where δ_{ij} is the Kronecker delta and the strain rates $\dot{\varepsilon}_{ij}$ are

$$\dot{\varepsilon}_{ij} = \frac{1}{2} \left(\frac{\partial v_i}{\partial x_j} + \frac{\partial v_j}{\partial x_i} \right) \tag{7}$$

In our work we will solve a *modified set of governing* equations derived using a finite calculus (FIC) formulation. The FIC governing equations are [ONA 98, ONA 00, ONA 01]

Momentum

$$r_{m_i} - \underline{\frac{1}{2} h_j \frac{\partial r_{m_i}}{\partial x_j}} = 0 \qquad [8]$$

Mass balance

$$r_d - \underline{\frac{1}{2} h_j \frac{\partial r_d}{\partial x_j}} = 0 \qquad [9]$$

The problem definition is completed with the following boundary conditions

$$n_j \sigma_{ij} - t_i + \underline{\frac{1}{2} h_j n_j r_{m_i}} = 0 \quad \text{on } \Gamma_t \qquad [10a]$$

$$v_j - v_j^p = 0 \quad \text{on } \Gamma_v \qquad [10b]$$

and the initial condition is $v_j = v_j^0$ for $t = t_0$. The standard sum convention for repeated indexes is assumed unless otherwise specified.

In [10a] and [10b] t_i and v_j^p are surface tractions and prescribed velocities on the boundaries Γ_t and Γ_v, respectively, n_j are the components of the unit normal vector to the boundary.

Eqs. [8], [9] and [10a] are obtained by invoking the standard balance laws in fluid mechanics (balance of mass, momentum and equilibrium of surface tractions) in a domain of finite size.

The $h_i's$ in above equations are *characteristic lengths* of the domain where balance is enforced. Details of the derivation of [7]–[10] can be found in [ONA 98, ONA 00, ONA 01, ONA 04B].

Eqs. [8]–[10] are the starting point for deriving stabilized finite element methods for solving the incompressible flow equations in a Lagrangian frame of reference using equal order interpolation for the velocity and pressure variables [IDE 02, IDE 03, IDE 03B, IDE 04, ONA 03, AUB 04]. Application of the FIC formulation to finite element and meshless analysis of fluid flow problems can be found in [GAR 03, ONA 00, ONA 03, ONA 04, ONA 00B, ONA 04C, ONA 01, ONA 98B].

Transformation of the mass balance equation. Integral governing equations. The underlined term in [9] can be expressed in terms of the momentum equations. The new expression for the mass balance equation is [ONA 04, ONA 04C]

$$r_d - \sum_{i=1}^{n_d} \tau_i \frac{\partial r_{m_i}}{\partial x_i} = 0 \qquad [11]$$

with

$$\tau_i = 3h_i^2/8\mu \qquad [12]$$

The τ_i's in [11], when scaled by the density, are termed *intrinsic time parameters*. Similar values for τ_i (usually $\tau_i = \tau$ is taken) are used in other works from ad-hoc extensions of the 1D advective-diffusive problem [COD 98, COD 00, COD 02, COD 02B,

CRU 97, CRU 99, DON 03, FRA 92, HAN 00, HUG 86, HUG 89, HUG 94, ONA 98, ONA 00, SHE 96, STO 04, TEZ 92, ZIE 00].

At this stage it is not longer necessary to retain the stabilization terms in the momentum equations. These terms are critical in Eulerian formulations to stabilize the numerical solution for high values of the convective terms. In the Lagrangian formulation the convective terms dissapear from the momentum equations and the FIC terms in these equations are just useful to derive the form of the mass balance equation given by [11] and can be disregarded there onwards. Consistenly, the stabilization terms are also neglected in the Neuman boundary conditions [10a].

The weighted residual expression of the final form of the momentum and mass balance equations can be written as

$$\int_\Omega \delta v_i r_{m_i} d\Omega + \int_{\Gamma_i} \delta v_i (n_j \sigma_{ij} - t_i) d\Gamma = 0 \qquad [13]$$

$$\int_\Omega q \Big[r_d - \sum_{i=1}^{n_d} \tau_i \frac{\partial r_{m_i}}{\partial x_i} \Big] d\Omega = 0 \qquad [14]$$

The computation of the residual terms in [14] can be simplified if we introduce now the pressure gradient projections π_i, defined as

$$\pi_i = r_{m_i} - \frac{\partial p}{\partial x_i} \qquad [15]$$

We express now r_{m_i} in [14] in terms of the π_i which then become additional variables. The system of integral equations is therefore augmented in the necessary number of equations by imposing that the residuals r_{m_i} vanish within the analysis domain (in an average sense). This gives the final system of governing equation (after substitution of [5] and [6] into [3] and integration by parts of the deviatoric stresses and the pressure terms) as:

$$\int_\Omega \left[\delta v_i \rho \frac{\partial v_i}{\partial t} + \delta \dot{\varepsilon}_{ij} (s_{ij} - \delta_{ij} p) \right] d\Omega - \int_\Omega \delta v_i b_i d\Omega - \int_{\Gamma_t} \delta v_i t_i d\Gamma = 0 \qquad [16]$$

$$\int_\Omega q \frac{\partial v_i}{\partial x_i} d\Omega + \int_\Omega \sum_{i=1}^{n_d} \tau_i \frac{\partial q}{\partial x_i} \left(\frac{\partial p}{\partial x_i} + \pi_i \right) d\Omega = 0 \qquad [17]$$

$$\int_\Omega \delta \pi_i \tau_i \left(\frac{\partial p}{\partial x_i} + \pi_i \right) d\Omega = 0 \qquad \text{no sum in } i \qquad [18]$$

with $i, j, k = 1, n_d$. In Eqs. [18] $\delta \pi_i$ are appropriate weighting functions and the τ_i weights are introduced for symmetry reasons.

4. Finite element discretization

We choose C° continuous interpolations of the velocities, the pressure and the pressure gradient projections π_i over each element with n nodes. The interpolations are written as

$$v_i = \sum_{j=1}^{n} N_j \bar{v}_i^j \quad , \quad p = \sum_{j=1}^{n} N_j \bar{p}^j \quad , \quad \pi_i = \sum_{j=1}^{n} N_j \bar{\pi}_i^j \qquad [19]$$

where $\bar{(\cdot)}^j$ denotes nodal variables and N_j are the shape functions [ZIE00]. More details of the mesh discretization process and the choice of shape functions are given in Section 8.

Substituting the approximations [19] into [16]–[18] and choosing a Galerking form with $\delta v_i = q = \delta \pi_i = N_i$ leads to the following system of discretized equations

$$\mathbf{M}\dot{\bar{\mathbf{v}}} + \bar{\mathbf{g}} - \mathbf{f} = \mathbf{0} \qquad [20a]$$

$$\mathbf{G}^T \bar{\mathbf{v}} + \mathbf{L}\bar{\mathbf{p}} + \mathbf{Q}\bar{\boldsymbol{\pi}} = \mathbf{0} \qquad [20b]$$

$$\mathbf{Q}^T \bar{\mathbf{p}} + \hat{\mathbf{M}}\bar{\boldsymbol{\pi}} = \mathbf{0} \qquad [20c]$$

where

$$\bar{\mathbf{g}} = \int_\Omega \mathbf{B}^T [\mathbf{s} - \mathbf{m}p] d\Omega \qquad [21]$$

is the internal nodal force vector derived from the momentum equations, $\mathbf{s}$ is the deviatoric stress vector, $\mathbf{B}$ is the strain rate matrix and $\mathbf{m} = [1, 1, 0]^T$ for 2D problems.

This vector and the rest of the matrices and vectors in Eqs. [20] are assembled from the element contributions given by (for 2D problems)

$$M_{ij} = \int_{\Omega^e} \rho N_i N_j d\Omega \quad , \quad \bar{\mathbf{g}}_i = \int_\Omega \mathbf{B}_i^T [\mathbf{s} - \mathbf{m}p] d\Omega \quad , \quad \mathbf{B}_i = \begin{bmatrix} \frac{\partial N_i}{\partial x_1} & 0 \\ 0 & \frac{\partial N_i}{\partial x_2} \\ \frac{\partial N_i}{\partial x_2} & \frac{\partial N_i}{\partial x_1} \end{bmatrix}$$

$$L_{ij} = \int_{\Omega^e} \tau_k \frac{\partial N_i}{\partial x_k} \frac{\partial N_j}{\partial x_k} d\Omega \quad , \quad \mathbf{Q} = [\mathbf{Q}^1, \mathbf{Q}^2] \quad , \quad Q_{ij}^k = \int_{\Omega^e} \tau_k \frac{\partial N_i}{\partial x_k} N_j d\Omega$$

$$\hat{\mathbf{M}} = \begin{bmatrix} \hat{\mathbf{M}}^1 & \mathbf{0} \\ \mathbf{0} & \hat{\mathbf{M}}^2 \end{bmatrix} \quad , \quad \hat{\mathbf{M}}_{ij}^k = \int_{\Omega^e} \tau_k N_i N_j d\Omega \quad , \quad \mathbf{G}_{ij} = \int_{\Omega^e} \mathbf{B}_i^T \mathbf{m} N_j d\Omega$$

$$\mathbf{f}_i = \int_{\Omega^e} N_i \mathbf{b} d\Omega + \int_{\Gamma^e} N_i \mathbf{t} d\Gamma \quad , \quad \mathbf{b} = [b_1, b_2]^T \quad , \quad \mathbf{t} = [t_1, t_2]^T \qquad [22]$$

with $i, j = 1, n$ and $k, l = 1, 2$. As usual the deviatoric stresses s_{ij} are related to the strain rates $\dot{\varepsilon}_{ij}$ by [6].

It can be shown that the system of Eqs. [20] leads to a stabilized numerical solution. For details see [ONA03].

5. Fractional step method for fluid-structure interaction analysis

A simple and effective iterative algorithm can be obtained by splitting the pressure from the momentum equations as follows

$$\bar{\mathbf{v}}^{*} = \bar{\mathbf{v}}^{n} - \Delta t \mathbf{M}^{-1}[\mathbf{g}^{n+\theta_1,j} - \mathbf{f}^{n+1}] \qquad [23a]$$

$$\bar{\mathbf{v}}^{n+1,j} = \bar{\mathbf{v}}^{*} + \Delta t \mathbf{M}^{-1}\mathbf{G}\delta\bar{\mathbf{p}} \qquad [23b]$$

In Eq. [23a]

$$\mathbf{g}^{n+\theta_1,j} = \int_{\Omega^{n+\theta_1,j}} \mathbf{B}^{T}[\mathbf{s}^{n+\theta_1,j} - \alpha \mathbf{m}^{T} p^{n}] d\Omega$$

and α is a variable taking values equal to zero or one. For $\alpha = 0$, $\delta p \equiv p^{n+1,j}$ and for $\alpha = 1$, $\delta p = \Delta p$. Note that in both cases the sum of [23a] and [23b] gives the time discretization of the momentum equations with the pressures computed at t^{n+1}. In above equations and in the following superindex j denotes the iteration number within each time step.

The value of $\bar{\mathbf{v}}^{n+1,j}$ from [23b] is substituted now into Eq.[20b] to give

$$\mathbf{G}^{T}\bar{\mathbf{v}}^{*} + \Delta t \mathbf{G}^{T}\mathbf{M}^{-1}\mathbf{G}\delta\bar{\mathbf{p}} + \mathbf{L}\bar{\mathbf{p}}^{n+1,j} + \mathbf{Q}\bar{\boldsymbol{\pi}}^{n+\theta_2,j} = 0 \qquad [24a]$$

The product $\mathbf{G}^{T}\mathbf{M}^{-1}\mathbf{G}$ can be approximated by a laplacian matrix, i.e.

$$\mathbf{G}^{T}\mathbf{M}^{-1}\mathbf{G} = \hat{\mathbf{L}} \quad \text{with } \hat{\mathbf{L}}_{ij} \simeq \int_{\Omega^e} \frac{1}{\rho} \boldsymbol{\nabla}^{T} N_i \boldsymbol{\nabla} N_j \, d\Omega \qquad [24b]$$

In above equations θ_1 and θ_2 are algorithmic parameters ranging between zero and one. A discussion of the choice of θ_1 and θ_2 is given below.

A semi-implicit algorithm can be derived as follows. For each iteration:

Step 1 Compute $\mathbf{v}^{*}$ from Eq.[23a] with $\mathbf{M} = \mathbf{M}_d$ where subscript d denotes hereonwards a diagonal matrix.

Step 2 Compute $\delta\bar{\mathbf{p}}$ and $\mathbf{p}^{n+1}$ from Eq.[24a] as

$$\delta\bar{\mathbf{p}} = -(\mathbf{L} + \Delta t\hat{\mathbf{L}})^{-1}[\mathbf{G}^{T}\bar{\mathbf{v}}^{*} + \mathbf{Q}\bar{\boldsymbol{\pi}}^{n+\theta_2,j} + \alpha\mathbf{L}\bar{\mathbf{p}}^{n}] \qquad [25a]$$

$$\mathbf{p}^{n+1,j} = \mathbf{p}^{n} + \delta\mathbf{p} \qquad [25b]$$

Step 3 Compute $\bar{\mathbf{v}}^{n+1,j}$ from Eq.[23b] with $\mathbf{M} = \mathbf{M}_d$

Step 4 Compute $\bar{\boldsymbol{\pi}}^{n+1,j}$ from Eq.[20c] as

$$\bar{\boldsymbol{\pi}}^{n+1,j} = -\hat{\mathbf{M}}_d^{-1}\mathbf{Q}^{T}\bar{\mathbf{p}}^{n+1,j} \qquad [26]$$

Step 5 Solve for the movement of the structure due to the fluid flow forces.

This implies solving the dynamic equations of motion for the structure written as

$$\mathbf{M}_s\ddot{\mathbf{d}} + \mathbf{K}_s\mathbf{d} = \mathbf{f}_{\text{ext}} \qquad [27]$$

where $\mathbf{d}$ and $\ddot{\mathbf{d}}$ are respectively the displacement and acceleration vectors of the nodes discretizing the structure, $\mathbf{M}_s$ and $\mathbf{K}_s$ are the mass and stiffness matrices of the structure and $\mathbf{f}_{\text{ext}}$ is the vector of external nodal forces accounting for the fluid flow forces induced by the pressure and the viscous stresses. Clearly the main driving forces for the motion of the structure is the fluid pressure which acts as normal a surface traction on the structure. Indeed [27] can be augmented with an appropriate damping term. The form of all the relevant matrices and vectors can be found in standard books on FEM for structural analysis [ZIE00].

Solution of [27] in time can be performed using implicit or fully explicit time integration algorithms. In both cases the values of the nodal displacements, velocities and accelerations of the structure at t^{n+1} are found for the jth iteration.

Step 6 Update the mesh nodes in a Lagrangian manner as

$$\mathbf{x}_i^{n+1,j} = \mathbf{x}_i^n + \bar{\mathbf{v}}_i^{n+1,j}\Delta t \qquad [28]$$

Step 7 Generate a new mesh. This is performed using the method described in Section 6.

Step 8 Check the convergence of the velocity and pressure fields in the fluid and the displacements strains and stresses in the structure. If convergence is achieved move to the next time step, otherwise return to step 1 for the next iteration with $j+1 \rightarrow j$.

Despite the motion of the nodes within the iterative process, in general there is no need to regenerate the mesh at each iteration. A new mesh is typically generated after a prescribed number of converged time steps, or when the nodal displacements induce significant geometrical distorsions in some elements. *In the examples presented in the paper the mesh in the fluid domain has been regenerated at each time step.*

The boundary conditions are applied as follows. No condition is applied in the computation of the fractional velocities $\mathbf{v}^*$ in [23a]. The prescribed velocities at the boundary are applied when solving for $\bar{\mathbf{v}}^{n+1,j}$ in step 3. The prescribed pressures at the boundary are imposed by making zero the pressure increments at the relevant boundary nodes and making $\bar{\mathbf{p}}^n$ equal to the prescribed pressure values. Details of the treatment of the contact conditions at the solid-fluid interface are given in the next Section [IDE04].

Note that solution of steps 1, 3 and 4 does not require the solution of a system of equations as a diagonal form is chosen for $\mathbf{M}$ and $\hat{\mathbf{M}}$. The whole solution process within a time step can be linearized by choosing $\theta_1 = \theta_2 = 0$ and now the iteration loop is no longer necessary. The implicit solution for $\theta_1 = \theta_2 = 1$ is however very

effective as larger time steps can be used. This requires some iterations within steps 1–8 until converged values for the fluid and solid variables and the new position of the mesh nodes at time $n+1$ are found.

In the examples presented in the paper the time increment size has been chosen as

$$\Delta t = \min(\Delta t_i) \quad \text{with} \quad \Delta t_i = \frac{|\mathbf{v}|}{h_i^{\min}} \qquad [29]$$

where $h_i^{\min}$ is the distance between node i and the closest node in the mesh.

REMARK 1. – Although not explicitely mentioned for $\theta_1 = 1$ all matrices and vectors in [26]–[28] are computed at the final configuration $\Omega^{n+1,j}$. This means that the integration domain changes for each iteration and, hence, all the terms involving space derivatives must be updated at each iteration. This problem dissapears if Ω^n is taken as the reference configuration ($\theta_1 = 0$) as this remains fixed during the iterations. The penalty to pay in this case, however, is the evaluation of the Jacobian matrix at each iteration [AUB04].

6. Treatment of contact between fluid and solid interfaces

The condition of prescribed velocities or pressures at the solid boundaries in the PFEM are applied in strong form to the boundary nodes. These nodes might belong to fixed external boundaries or to moving boundaries linked to the interacting solids. In some problems it is useful to define a layer of nodes adjacent to the external boundary in the fluid where the condition of prescribed velocity is imposed. These nodes typically remain fixed during the solution process. Contact between water particles and the solid boundaries is accounted for by the incompressibility condition which *naturally prevents the water nodes to penetrate into the solid boundaries*. This simple way to treat the water-wall contact is another attractive feature of the PFEM formulation.

7. Generation of a New Mesh

One of the key points for the success of the Lagrangian flow formulation described here is the fast regeneration of a mesh at every time step on the basis of the position of the nodes in the space domain. In our work the mesh is generated using the so called extended Delaunay tesselation (EDT) presented in [IDE03, IDE03C, IDE04]. The EDT allows one to generate non standard meshes combining elements of arbitrary polyhedrical shapes (triangles, quadrilaterals and other polygons in 2D and tetrahedra, hexahedra and arbitrary polyhedra in 3D) in a computing time of order n, where n is the total number of nodes in the mesh. The C° continuous shape functions of the elements can be simply obtained using the so called meshless finite element interpolation (MFEM) [IDE03, IDE03C, IDE04].

8. Identification of boundary surfaces

One of the main tasks in the PFEM is the correct definition of the boundary domain. Sometimes, boundary nodes are explicitly identified differently from internal nodes. In other cases, the total set of nodes is the only information available and the algorithm must recognize the boundary nodes.

Considering that the nodes follow a variable $h(x)$ distribution, where $h(x)$ is the minimum distance between two nodes, the following criterion has been used. *All nodes on an empty sphere with a radius greater than αh, are considered as boundary nodes*. In practice, α is a parameter close to, but greater than one. This criterion coincides with the Alpha Shape concept [EDE99].

Once a decision has been made concerning which nodes are on the boundaries, the boundary surface must be defined. In this work, the boundary surface is defined by all the polyhedral surfaces (or polygons in 2D) having all their nodes on the boundary and belonging to just one polyhedron.

The method described also allows to identify isolated fluid particles outside the main fluid domain. These particles are treated as part of the external boundary where the pressure is fixed to the atmospheric value.

Figure 1 shows a schematic example of the process to identify individual particles (or a group of particles) starting from a given collection of nodes.

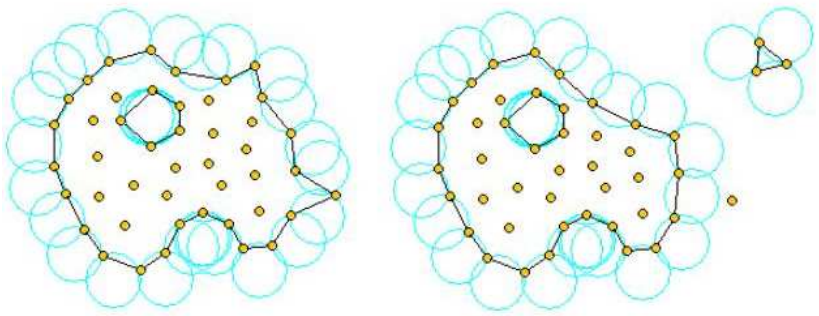

Figure 1. *Identification of individual particles (or a group of particles) starting from a given collection of nodes*

9. Modelling a rigid structure as a viscous fluid

A simple and yet effective way to analyze the rigid motion of solid bodies in fluids with the Lagrangian flow description is to model the solid as a fluid with a viscosity much higher than that of the surrounding fluid. The fractional step scheme of Section 6 can be readily applied skipping now step 5 and solving now for the simultaneous

motion of both fluid domains (the actual fluid and the fictitious fluid modelling the quasi-rigid body). Examples of this type are presented in Sections 10.3 and 10.4.

Indeed this approach can be further extended to account for the elastic deformation of the solid treated now as a visco-elastic fluid. This will however introduce some complexity in the formulation and the full coupled FSI scheme described in Section 5 is preferable.

10. Examples

The examples chosen show the applicability of the PFEM to solve problems involving large fluid motions and FSI situations. The fractional step algorithm of Section 5 with $\theta_2 = 1$ and $\alpha = 1$ has been used in all cases.

In examples 11.1–11.7 a value of $\theta_1 = 1$ has been chosen. This basically means that the final configuration $\Omega^{n+1,j}$ has been taken as the reference configuration at each iteration. In example 11.8 $\theta_1 = 0$ has been selected and, hence, the initial configuration Ω^n has been taken as a fixed reference configuration for all the iterations within a time step.

10.1. *Collapse of a water column*

The first problem solved to show the potential of the PFEM is the study of the collapse of a water column. This problem was solved in [KOS 96] both experimentally and numerically. It has became a classical example to validate the Lagrangian formulation for fluid flows. The water is initially kept within a rectangular container including a removable vertical board. A double layer of nodes in the solid walls is used in order to prevent water nodes from exiting the analysis domain. The boundary conditions impose zero velocity at the wall nodes and zero (atmospheric) pressure at the free surface. Figures 2b and 2c show the mesh discretizing the water domain and the solid walls at two different times of the analysis. The method allows one to follow the large motion of the water particles including separation of some water drops. The collapse starts at time t = 0, when the board is removed. Viscosity and surface tension are neglected in the analysis. Figures 2 and 3 show the point positions at different time steps. The dark points represent the free-surface detected with the algorithm described in Section 8. The internal points are shown in a gray colour and the fixed points in black.

Figure 4 shows the finite element mesh generated at a time step. We recall that this mesh is used to solve the equations of motion of the fluid particles as described in the previous sections.

The water is running on the bottom wall until, at 0.3 sec it impinges on the right vertical wall. Breaking waves appear at 0.6 sec. At about 1 sec. the wave again

reaches the left wall. Agreement with the experimental results of [KOS96] both in the shape of the free surface as well as in its time evolution are excellent.

The 3D solution of the same problem is shown in Figure 5. More information on the PFEM solution of this problem can be found in [IDE 04].

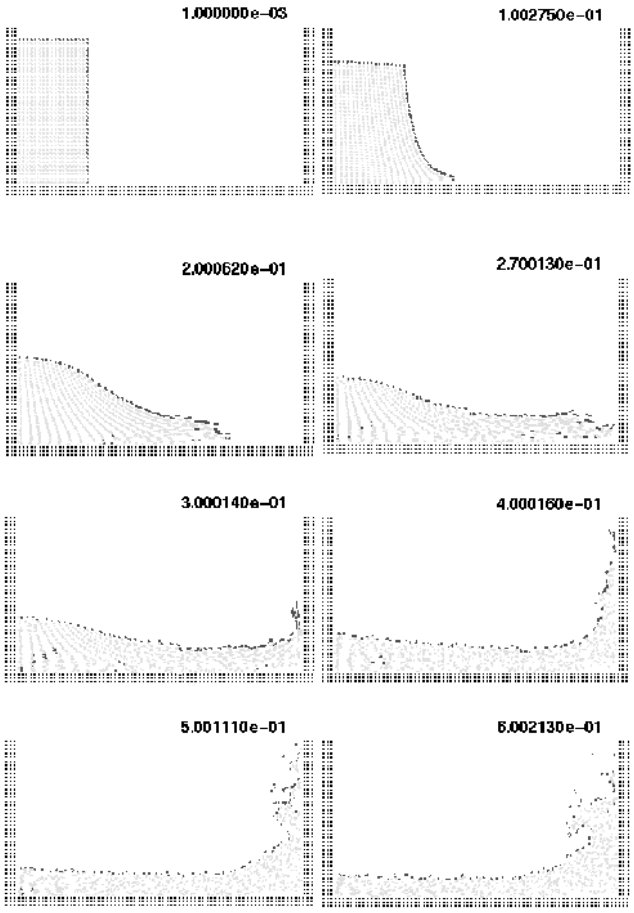

Figure 2. *Water column collapse at different time steps*

10.2. *Sloshing problems*

The simple problem of the free oscillation of an incompressible liquid in a container is considered next. Numerical solutions for this problem can be found in several references [RAD98]. This problem is interesting because there is an analytical solution for small amplitudes. Figure 6 shows a schematic view of the problem and the

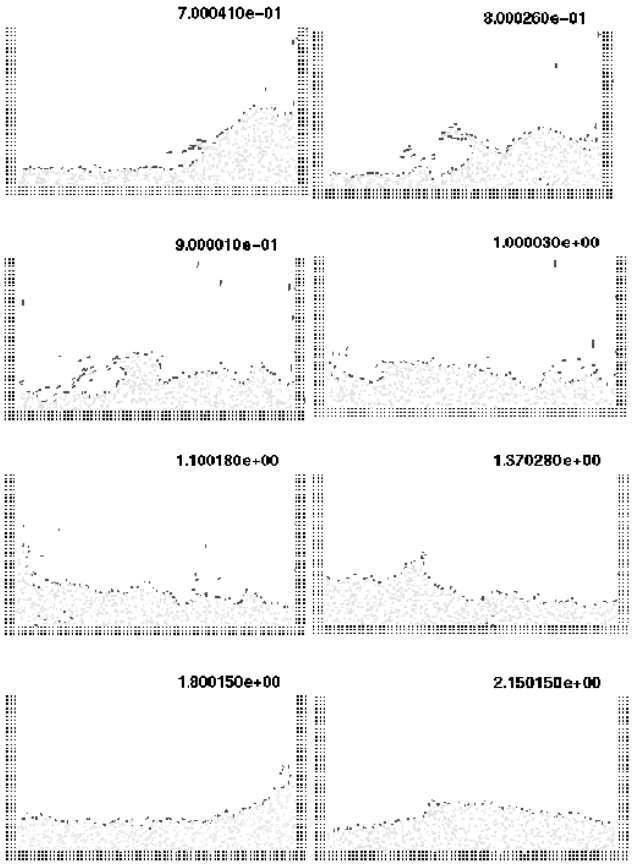

Figure 3. *Water column collapse at different time steps (continued)*

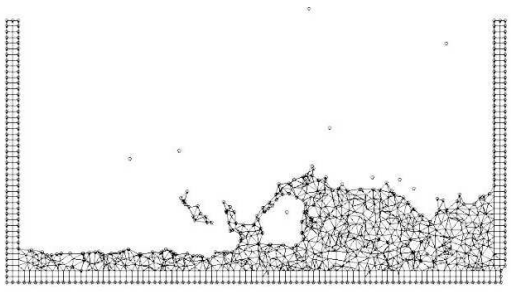

Figure 4. *Finite element mesh discretizing the fluid domain and the container walls at a certain time step*

point distribution in the initial position. The dark points represent the fixed points on the walls where the velocity is fixed to zero.

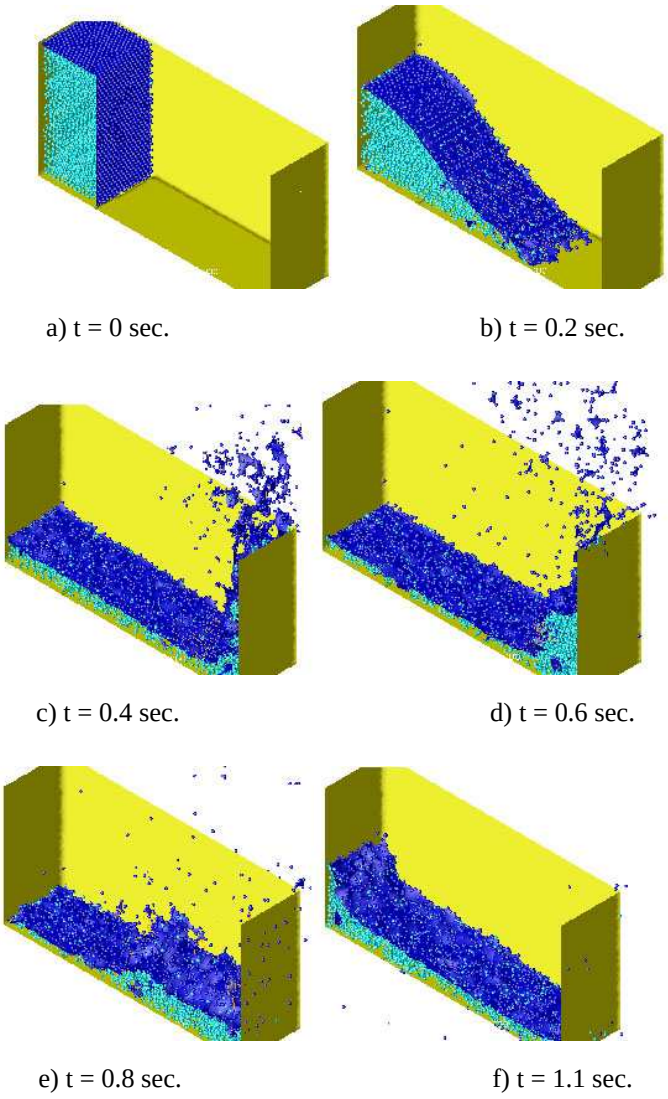

a) t = 0 sec. b) t = 0.2 sec.

c) t = 0.4 sec. d) t = 0.6 sec.

e) t = 0.8 sec. f) t = 1.1 sec.

Figure 5. *Water column collapse in a 3D domain*

Figure 6 shows the time evolution of the amplitude compared with the analytical results for the near inviscid case. Little numerical viscosity is observed on the phase wave and amplitude in spite of the relative poor point distribution.

The analytical solution is only acceptable for small wave amplitudes. For larger amplitudes, additional waves are overlapping and, finally, the wave breaks and also

some particles separate from the fluid domain due to their large velocity. Figure 7 shows the numerical results obtained with the PFEM for larger sloshing amplitudes. Breaking waves as well as separation effects can be seen on the free-surface. This particular and very complicated effect is well represented by the PFEM.

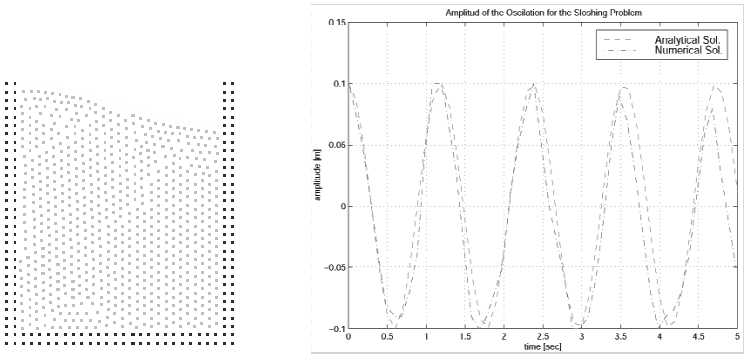

Figure 6. *Sloshing. Initial point distribution and comparison of the numerical and analytical solutions*

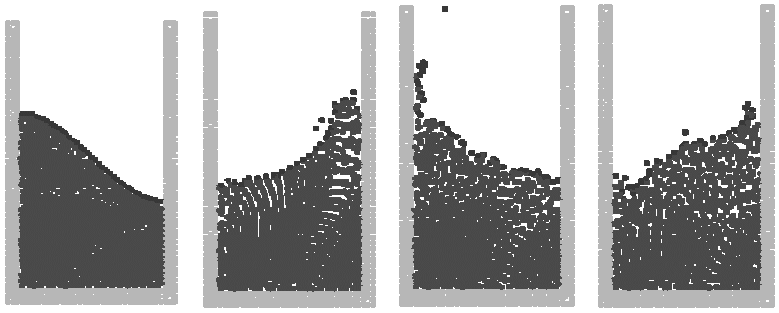

Figure 7. *PFEM results for a large amplitude sloshing problem*

In order to test the potentiality of the PFEM in a 3D domain, the same sloshing problem was solved in 3D. Figure 8 shows the different point positions at two time steps. Each point position was represented by a sphere and only a half of the fixed recipient is represented on the figure. This sphere representation is only used in order to improve the visualization of the numerical results.

10.3. *Wave breaking on a beach*

The initial position of the wave was given an oblique angle with the beach line. In this way, 3D effects show more clearly. When the wave hits the slope, the crest

of the wave accelerates differently accordingly with the depth, inducing the wave to correct its oblique position and break parallel to the beach. The results may be seen in Figure 9 for different time steps. The 2D solution of a similar problems is reported in [ONA04C].

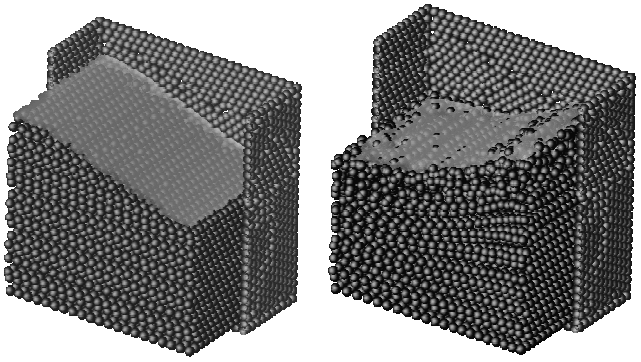

Figure 8. *3D sloshing problem*

10.4. *Fixed ship hit by wave*

This example is a very schematic representation of a ship when is hit by a big wave (Figure 10). The ship can not move and initially the free-surface near the ship is horizontal. Fixed nodes represent the ship as well as the domain walls. The example tests the suitability of the PFEM to solve water-wall contact situations even in the presence of curved walls. Note the breaking and splashing of the waves under the ship prow and the rebound of the incoming wave. It is also interesting to see the different water-wall contact situations at the internal and external ship surfaces and the moving free-surface at the back of the ship.

10.5. *Semi-submerged rotating water mill*

The example shown in Figure 11 is the analysis of a rotating water mill semi-submerged in water. The blades of the mill are treated as a rigid body with an imposed rotating velocity, while the water is initially in a stationary flat position. Fluid structure interactions with free-surfaces and water fragmentation are well reproduced in this example.

10.6. *Floating wood piece*

The next example shows an initially stationary recipient with a floating piece of wood where a wave is produced on the left side. The wood has been simulated by

a liquid of higher viscosity as described in Section 9. The wave intercepts the wood piece producing a breaking wave and displacing the floating wood as shown in Figure 12.

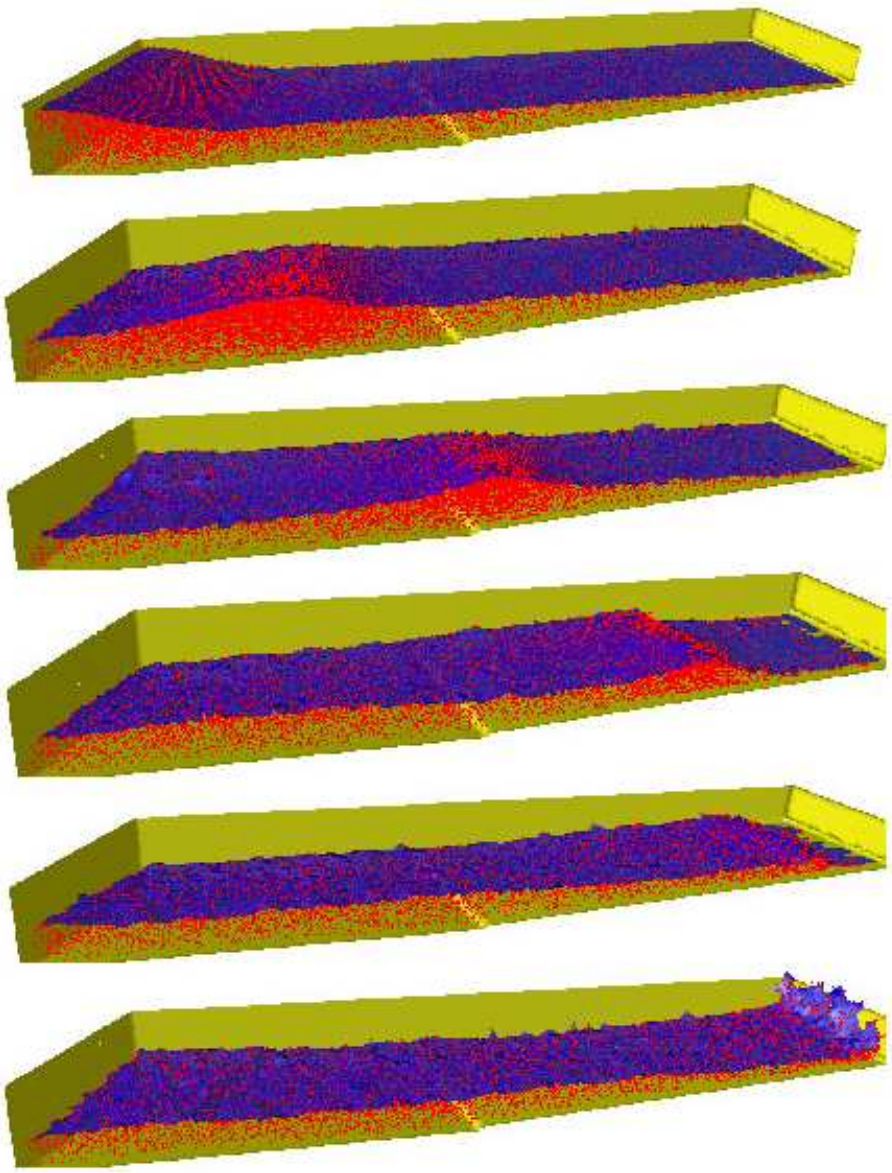

Figure 9. *Oblique breaking wave on a 3D domain*

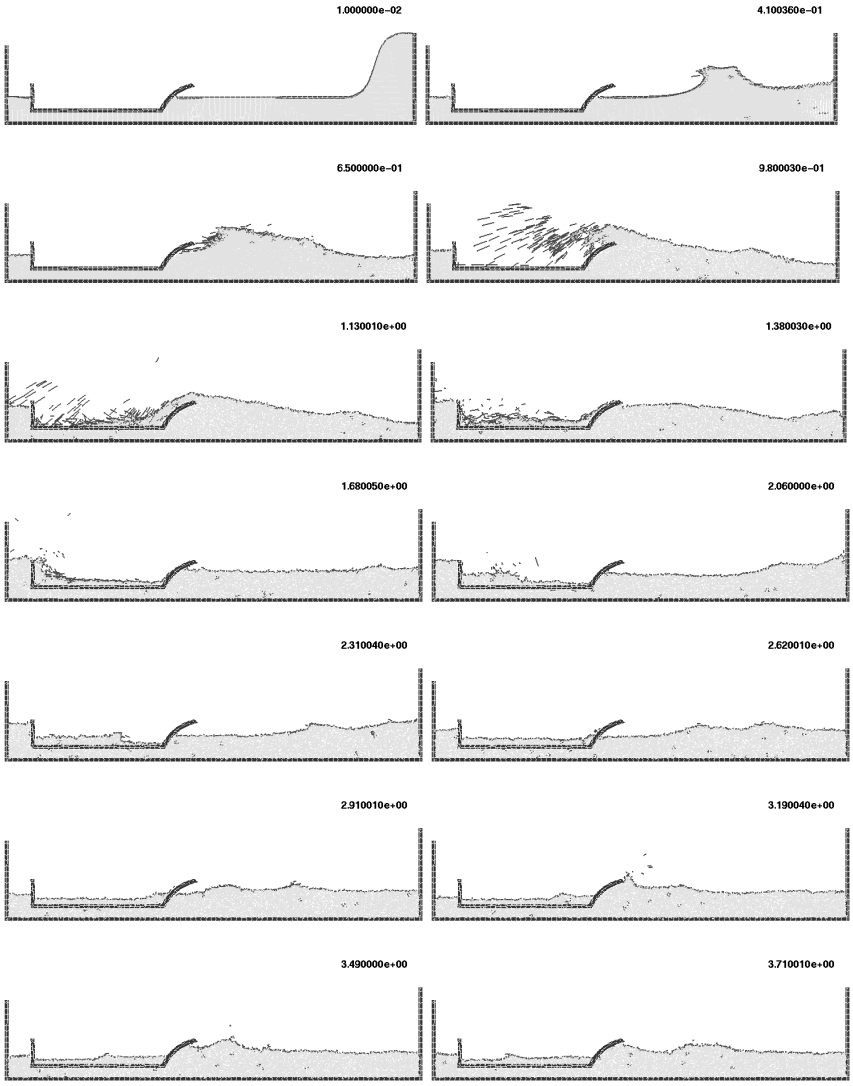

Figure 10. *Fixed ship hit by incoming wave*

10.7. *Container ship hit by an incoming wave*

Figure 13 shows the analysis of the motion of the transverse sections of a container ship hit by an incoming wave. The dynamic motion of the ship is induced by the resul-

tant of the pressure and the viscous forces acting on the ship boundaries. The section of the ship analyzed corresponds now to that of a real container ship. Differently to the case of Section 11.4 the rigid ship is free to move laterally due to the sea wave forces. The objective of the study was to asses the influence of the stabilizers in the ship roll. The figures show clearly how the PFEM predicts the ship and wave motions in a realistic manner.

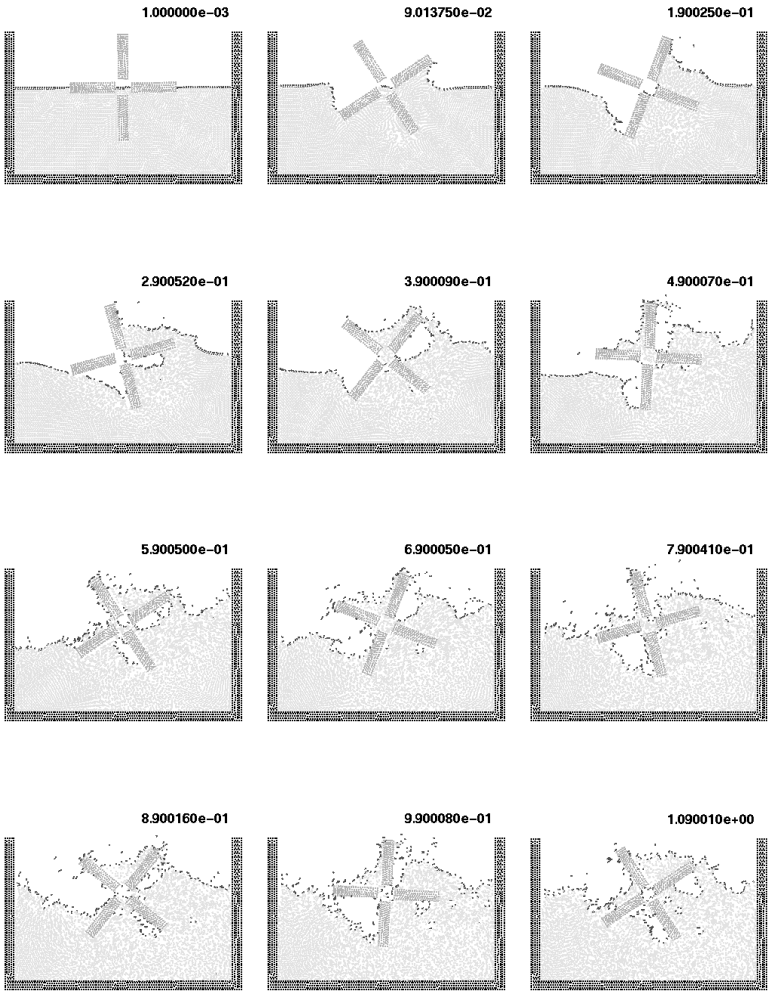

Figure 11. *Rotating water mill*

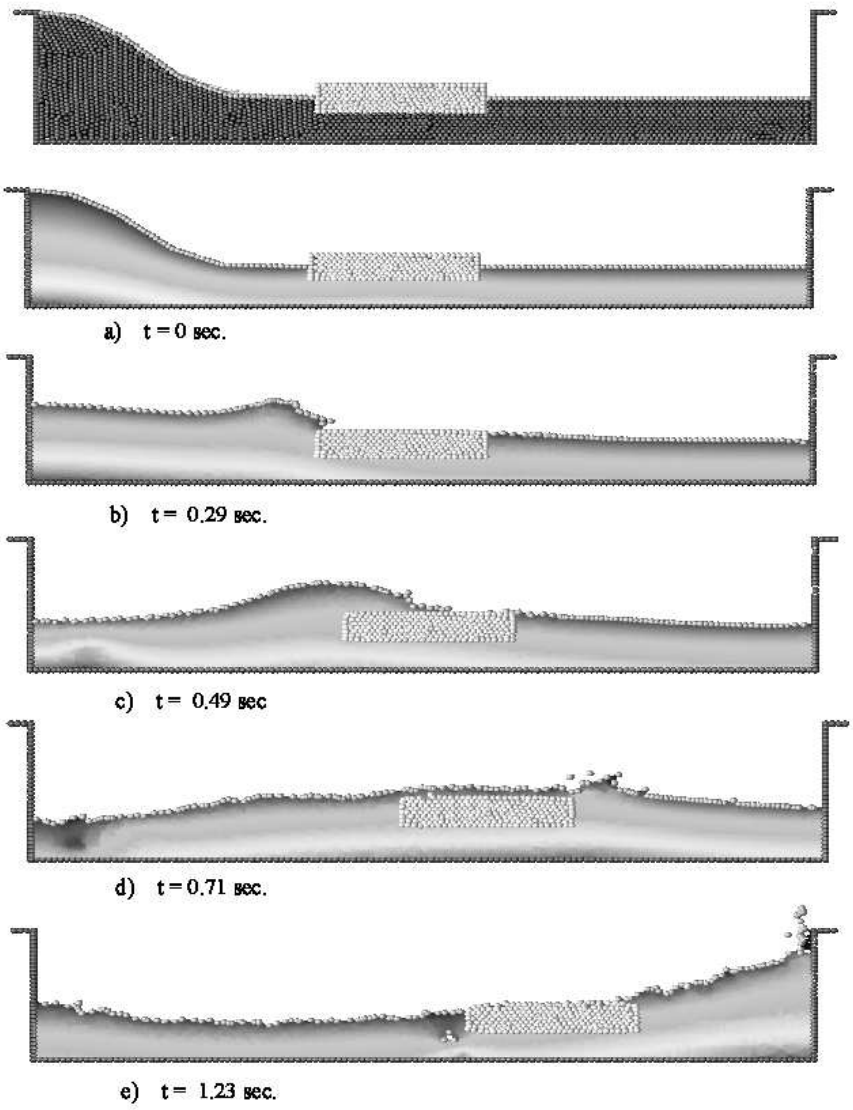

Figure 12. *Floating wood piece hit by a wave*

10.8. *Rigid cube falling in a recipient with water*

In the next example a solid cube is initially free and falls down within a water recipient. In this example, the rigid solid is modeled first as a fictitious fluid with a higher viscosity, similarly as for the floating solid of Section 11.6. The results of this analysis are shown in Figure 14. Note that the method reproduces very well the interaction of the cube with the free surface as well as the overall sinking process. A

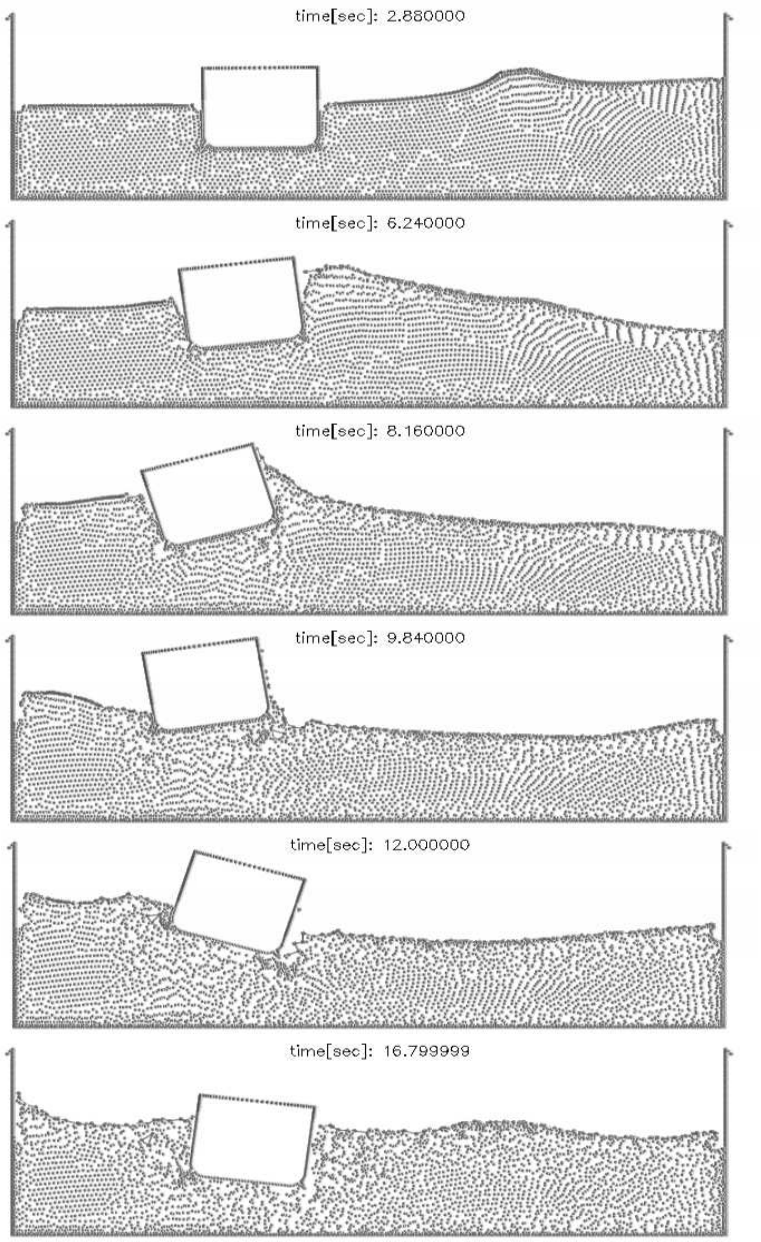

Figure 13. *Ship with stabilizers hit by a lateral wave*

small deformation of the cube is produced. This can be reduced by increasing further the fictitious viscosity of the cube particles.

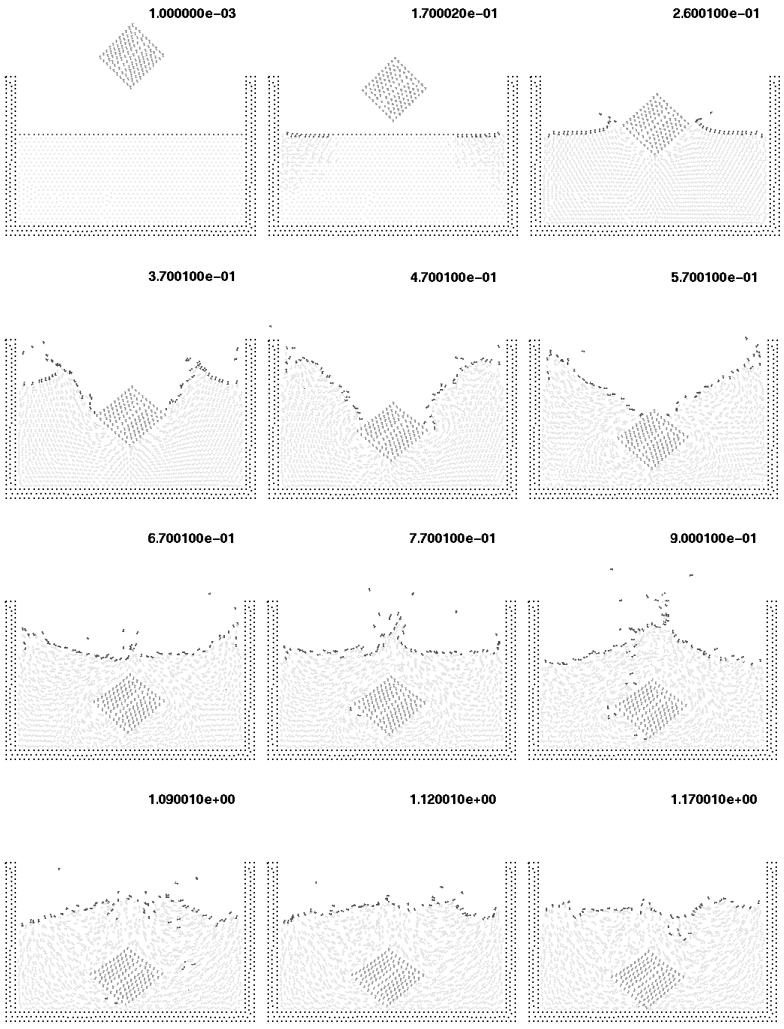

Figure 14. *Solid cube falling into a recipient with water. The cube is modelled as a very viscous fluid*

The same problem is analyzed again considering now the cube as a rigid solid subjected to pressure and viscous forces acting in its boundaries. The resultant of the

fluid forces and the weight of the cube are applied to the center of the cube. These forces govern the displacement of the cube which is computed by solving the dynamic equations of motion as described in the fractional step algorithm of Section 6, similarly as for the rigid ships of the previous example. Here again the moving cube contours define a boundary condition for the fluid particles at each time step.

Initially the solid falls down freely due to the gravity forces (Figure 15). Once in contact with the water surface, the Alpha-Shape method recognizes the different boundary contours which are shown with a thick line in the figure. The pressure and viscous forces are evaluated in all the domain and in particular on the cube contours. The fluid forces introduce a negative acceleration in the vertical motion until, once the cube is completely inside the water, the vertical velocity becomes zero. Then, buoyancy forces bring the cube up to the free-surface. It is interesting to observe that there is a rotation of the cube. The reason is that the center of the floating forces is higher in the rotated position than in the initial ones.

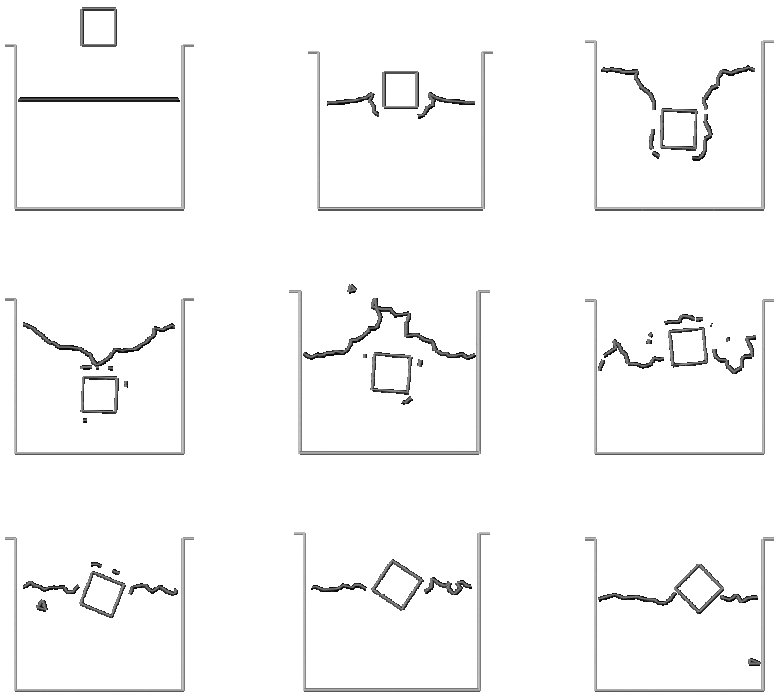

Figure 15. *Cube falling into a recipient with water. The cube is modelled as a rigid solid. Motion of the cube and free surface positions at different time steps*

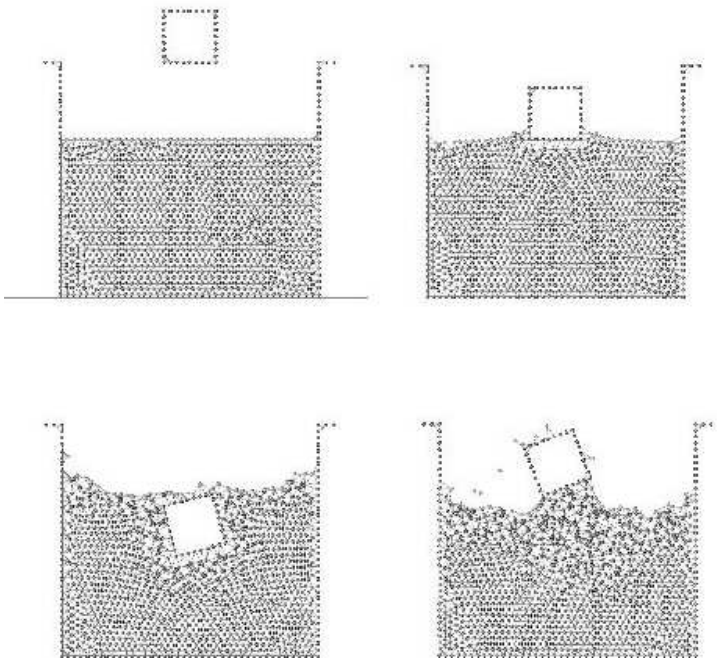

Figure 16. *Cube falling in a water recipient. The cube is modeled as a rigid solid. The finite element meshes generated at the selected instants are shown*

Figure 16 shows a repetition of the same problem showing now all the finite elements in the mesh discretizing the fluid. We recall that in all the problems here described the mesh in the fluid domain *is regenerated at each time step* combining linear triangles and quadrilateral elements as described in Section 8. Note that some fluid particles separate from the fluid domain. These particles are treated as free boundary points with zero pressure and hence fall down due to gravity.

It is interesting to see that the final position of the cube is different from that of Figure 15. This is due to the unstable character of the cube motion. A small difference in the numerical computations (for instance in the mesh generation process) shifts the movement of the cube towards the right or the left. Note that a final rotated equilibrium position is found in both cases.

10.9. *The Rayleigh-Bénard instability*

This example shows that the PFEM can also be successfully used to solve fluid flow problems traditionally analyzed with Eulerian formulations. The problem solved is that of a heated thin cavity containing a fluid. The flow pattern yields the so called Rayleigh-Bénard hydrodynamical instability giving a roll pattern along the cavity. In

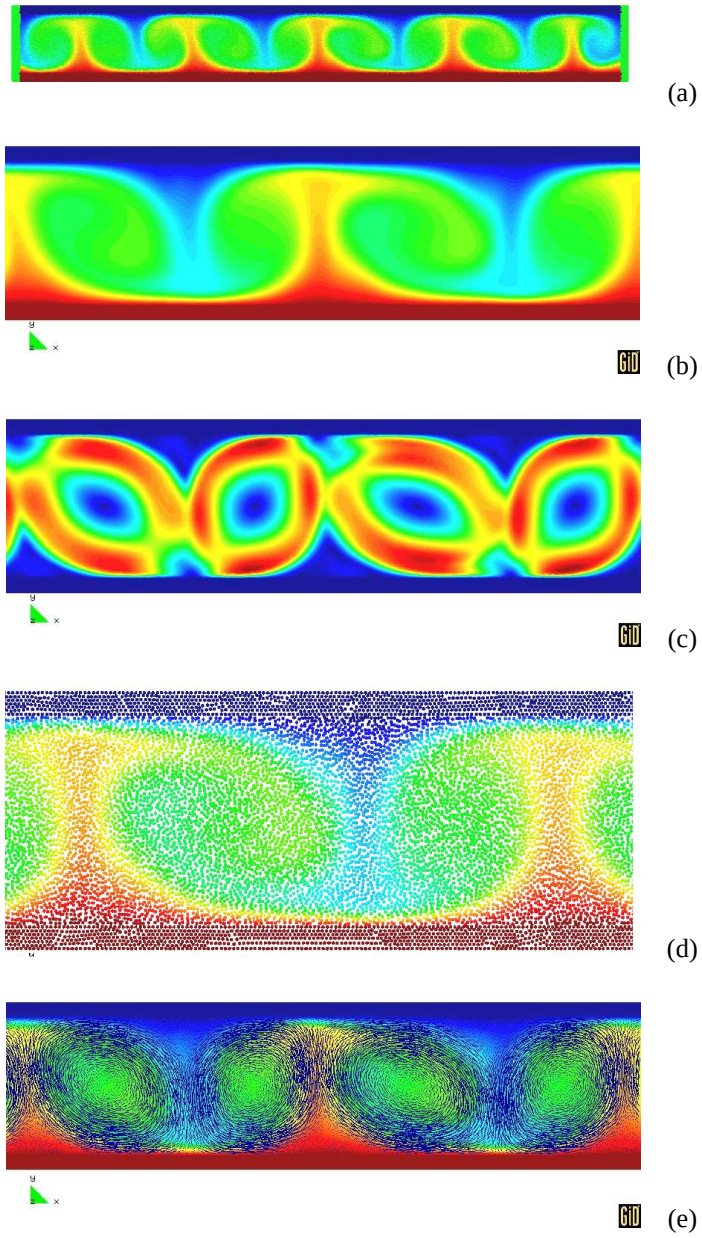

Figure 17. *Rayleigh-Bénard instability with $Ra = 10^5$ and $Pr = 10^{-1}$. (a) Temperature field. (b) Detail of temperature field. (c) Velocity norm field. (d) Detail of velocity norm field plotted on each particle. (e) Velocity vectors on temperature field*

this case the Lagrangian fluid flow equations are solved together with the heat transfer equation also written in a Lagrangian manner. As mentioned at the introduction of Section 10 a value of $\theta_1 = 0$ has been taken in this example. Details of the solution scheme using a Boussinesq approximatlions for the coupling between the heat transfer equation and the flow equations are given in [AUB04].

The bottom and upper part are isothermal with a temperature of 21° C for the bottom and 19° C for the top. The initial and reference temperature in the fluid is 20° C and the side parts are adiabatic. The Rayleigh and Prandtl numbers are 10^5 and 10^{-1}. The mesh has 35500 nodes and 69700 elements at the beginning of the analysis. The numerical computations start with the fluid at rest as the initial conditions. For rigid-rigid boundary conditions, the critical value of the Rayleigh number is 1708 so that the flow is here supercritical. However, a quasi-steady state is reached, with periodic oscillations of the temperature and the cells. Figure 17 shows results of the temperature and velocity field showing the development of rolls. Numerical results have been plotted using the GiD pre/postprocessing system developed at CIMNE [GID04]. More details on the application of the PFEM to this problem can be found in [AUB04].

11. Conclusions

The particle finite element method (PFEM) seems ideal to treat problems involving fluids with free surface and submerged or floating structures within a unified Lagrangian finite element framework. Problems such as the analysis of fluid-structure interactions, large motion of fluid or solid particles, surface waves, water splashing, separation of water drops, etc. can be easily solved with the PFEM. The success of the method lies in the accurate and efficient solution of the equations of an incompressible fluid and of solid dynamics using a stabilized finite element method via a fractional step scheme allowing the use of low order elements with equal order interpolation for all the variables. Other essential solution ingredients are the efficient regeneration of the finite element mesh using an extended Delaunay tesselation, the meshless finite element interpolation (MFEM) and the identification of the boundary nodes using an Alpha Shape type technique. The examples presented have shown the potential of the PFEM for solving a wide class of practical FSI problems.

Acknowledgements

Thanks are given to Prof. R.L. Taylor for many useful suggestions and to Mr. Nestor Calvo for this help in the development of the mesh generation process using the extended Delaunay technique.

12. References

[AUB 04] AUBRY R., IDELSOHN S.R., OÑATE E., "Particle finite element method in fluid mechanics including thermal convection-diffusion", *Computer & Structures*, submitted, 2004.

[CHO 67] CHORIN, A.J., "A numerical solution for solving incompressible viscous flow problems", *J. Comp. Phys.*, vol. 2, 1967, p. 12–26.

[COD 02] CODINA R., "Stabilized finite element approximation of transient incompressible flows using orthogonal subscales", *Comp. Meth. Appl. Mech. Engng.*, vol. 191, 2002, p. 4295–4321.

[COD 98] CODINA R., VAZQUEZ M., ZIENKIEWICZ O.C., "A general algorithm for compressible and incompressible flow - Part III. The semi-implicit form", *Int. J. Num. Meth. in Fluids*, vol. 27, 1998, p. 13–32.

[COD 00] CODINA R., BLASCO J., "Stabilized finite element method for the transient Navier-Stokes equations based on a pressure gradient operator", *Comp. Meth. in Appl. Mech. Engng.*, vol. 182, 2000, p. 277–301.

[COD 02B] CODINA R., ZIENKIEWICZ O.C., "CBS versus GLS stabilization of the incompressible Navier-Stokes equations and the role of the time step as stabilization parameter", *Communications in Numerical Methods in Engineering*, vol. 18, 2002, p. 99–112.

[CRU 97] CRUCHAGA M.A., OÑATE E., "A finite element formulation for incompressible flow problems using a generalized streamline operator", *Comp. Meth. Appl. Mech. Engng.*, vol. 143, 1997, p. 49–67.

[CRU 99] CRUCHAGA M.A., OÑATE E., "A generalized streamline finite element approach for the analysis of incompressible flow problems including moving surfaces", *Comp. Meth. Appl. Mech. Engng.*, vol. 173, 1999, p. 241–255.

[DON 03] DONEA J., HUERTA A., *Finite element method for flow problems*. J. Wiley, 2003.

[EDE 99] EDELSBRUNNER H., MUCKE E.P., "Three-dimensional alpha shapes", *ACM Trans. Graphics*, vol. 13, 1999, p. 43–72.

[FRA 92] FRANCA L.P., FREY S.L., "Stabilized finite element methods: II. The incompressible Navier-Stokes equations", *Comp. Meth. Appl. Mech. Engng.*, vol. 99, 1992, p. 209–233.

[GAR 03] GARCÍA J., OÑATE E., "An unstructured finite element solver for ship hydrodynamic problems", *J. Appl. Mech.*, vol. 70, 2003, p. 18–26.

[GID 04] "GiD. The personal pre/postprocessor", CIMNE, Barcelona, www.gidhome.com, 2004.

[HAN 90] HANSBO P., SZEPESSY A., "A velocity-pressure streamline diffusion finite element method for the incompressible Navier-Stokes equations", *Comp. Meth. Appl. Mech. Engng.*, vol. 84, 1990, p. 175–192.

[HUG 86] HUGHES T.J.R., FRANCA L.P., BALESTRA M., "A new finite element formulation for computational fluid dynamics. V Circumventing the Babuska-Brezzi condition: A stable Petrov-Galerkin formulation of the Stokes problem accomodating equal order interpolations", *Comp. Meth. Appl. Mech. Engng.*, vol. 59, 1986, p. 85–89.

[HUG 89] HUGHES T.J.R., FRANCA L.P., HULBERT G.M., "A new finite element formulation for computational fluid dynamics: VIII. The Galerkin/least-squares method for advective-diffusive equations", *Comp. Meth. Appl. Mech. Engng.*, vol. 73, 1989, p. 173–189.

[HUG 94] HUGHES T.J.R., HAUKE G., JANSEN K., "Stabilized finite element methods in fluids: Inspirations, origins, status and recent developments", in: *Recent Developments in Finite Element Analysis*. A Book Dedicated to Robert L. Taylor, T.J.R. Hughes, E. Oñate and O.C. Zienkiewicz (Eds.), CIMNE, Barcelona, Spain, p. 272–292, 1994.

[IDE 02] IDELSOHN S.R., OÑATE E., DEL PIN F., CALVO N., "Lagrangian formulation: the only way to solve some free-surface fluid mechanics problems", *Fith World Congress on Computational Mechanics*, Mang HA, Rammerstorfer FG and Eberhardsteiner J. (eds), Vienna, Austria, 2002.

[IDE 03] IDELSOHN S.R., OÑATE E., CALVO N., DEL PIN F., "The meshless finite element method", *Int. J. Num. Meth. Engng.*, vol. 58, 2003, p. 893–912.

[IDE 03B] IDELSOHN S.R., OÑATE E., DEL PIN F., "A lagrangian meshless finite element method applied to fluid-structure interaction problems", in *Computer and Structures*, vol. 81, 2003, p. 655–671.

[IDE 03C] IDELSOHN S.R., CALVO N., OÑATE E., "Polyhedrization of an arbitrary point set", *Comp. Meth. Appl. Mech. Engng.*, vol. 192, 2003, p. 2649–2668.

[IDE 04] IDELSOHN S.R., OÑATE E., DEL PIN F., "The particle finite element method, a powerful tool to solve incompressible flows with free-surfaces and breaking waves", *Int. J. Num. Meth. Engng.*, submitted, 2004.

[KOS 96] KOSHIZUKA S., OKA Y., "Moving particle semi-implicit method for fragmentation of incompressible fluid", *Nuclear Engng. Science*, vol. 123, 1996, p. 421–434.

[LAI 60] LAITONE E.V., "The second approximation to cnoidal waves", *J. Fluids Mech.*, vol. 9, 1960, p. 430.

[ONA 98] Oñate E., "Derivation of stabilized equations for advective-diffusive transport and fluid flow problems", *Comp. Meth. Appl. Mech. Engng.*, vol. 151, 1998, p. 233–267.

[ONA 98B] OÑATE E., IDELSOHN S.R., "A mesh free finite point method for advective-diffusive transport and fluid flow problems", *Comp. Mech.*, vol. 21, 1998, p. 283–292.

[ONA 00] OÑATE E., "A stabilized finite element method for incompressible viscous flows using a finite increment calculus formulation", *Comp. Meth. Appl. Mech. Engng.*, vol. 182, 2000, p. 355–370.

[ONA 00B] OÑATE E., SACCO C., IDELSOHN S.R., "A finite point method for incompressible flow problems", *Comput. and Visual. in Science*, vol. 2, 2000, p. 67–75.

[ONA 01] OÑATE E., GARCÍA J., "A finite element method for fluid-structure interaction with surface waves using a finite calculus formulation", *Comp. Meth. Appl. Mech. Engng.*, vol. 191, 2001, p. 635–660.

[ONA 03] OÑATE E., IDELSOHN S.R., DEL PIN F., "Lagrangian formulation for incompressible fluids using finite calculus and the finite element method", in *Numerical Methods for Scientific Computing Variational Problems and Applications*, Y. Kuznetsov, P. Neittanmaki and O. Pironneau (Eds.), CIMNE, Barcelona, 2003.

[ONA 04] OÑATE E., "Possibilities of finite calculus in computational mechanics", *Int. J. Num. Meth. Engng.*, vol. 60, 2004, p. 255-281.

[ONA 04B] OÑATE E., ROJEK J., TAYLOR R.L ZIENKIEWICZ O.C., "Finite calculus formulation for incompressible solids using linear triangles and tetraedra", *Int. J. Num. Meth. Engng.*, vol. 59, 2004, p. 1473-1500.

[ONA 04C] OÑATE E., GARCÍA J., IDELSOHN S.R., "Ship hydrodynamics", In *Encyclopedia of Computational Mechanics*, E. Stein, R. de Borst and T.J.R. Hughes (Eds), J. Wiley, 2004.

[RAD 98] RADOVITZKI R., ORTIZ M., "Lagrangian finite element analysis of Newtonian flows", *Int. J. Num. Meth. Engng.*, vol. 43, 1998, p. 607–619.

[SHE 96] SHENG C., TAYLOR L.K., WHITFIELD D.L.,"Implicit lower-upper / approximate-factorization schemes for incompressible flows", *J. Comp. Phys.*, vol. 128, 1996, p. 32–42.

[STO 95] STORTI M., NIGRO N., IDELSOHN S.R., "Steady state incompressible flows using explicit schemes with an optimal local preconditioning", *Comp. Meth. Appl. Mech. Engng.*, vol. 124, 1995, p. 231–252.

[TEZ 92] TEZDUYAR T.E., MITTAL S., RAY S.E., SHIH R.,"Incompressible flow computations with stabilized bilinear and linear equal order interpolation velocity–pressure elements", *Comput. Methods Appl. Mech. Engng.*, vol. 95, 1992, p. 221–242.

[ZIE 00] ZIENKIEWICZ O.C., TAYLOR R.L. *The finite element method*, 2000, 5th Edition, 3 Volumes, Butterworth–Heinemann.